

Predicting the Turbulent Air-Sea Surface Fluxes, Including Spray Effects, from Weak to Strong Winds

Edgar L Andreas
NorthWest Research Associates, Inc.
25 Eagle Ridge
Lebanon, New Hampshire 03766-1900
phone: (603) 448-3555 fax: (603) 448-3555 email: eandreas@nwra.com

Larry Mahrt
NorthWest Research Associates, Inc.
2171 NW Kari
Corvallis, Oregon 97330
phone: (541) 754-7501 fax: (541) 737-2540 email: mahrt@nwra.com

Contract Number: N00014-11-1-0073
<http://www.nwra.com/>

LONG-TERM GOALS

The goal is to investigate, through theory and by analyzing existing data, sea surface physics and air-sea exchange in winds that range from weak to hurricane-strength. Ultimately, we want to develop unified parameterizations for the fluxes of momentum, sensible and latent heat, and enthalpy across the air-sea interface. These flux parameterizations will provide improved model coupling between the ocean and the atmosphere and, in essence, set the lower flux boundary conditions on atmospheric models and the upper flux boundary conditions on ocean models.

OBJECTIVES

1. Develop a theoretical framework for predicting air-sea fluxes from mean meteorological conditions and apply uniform analyses, based on this framework, to datasets that we will assemble.
2. Assemble a large collection of quality air-sea flux data that represents a wide variety of conditions.
3. Compute fluxes from these datasets using an improved analysis that better accommodates measurements made over heterogeneous surfaces, such as coastal zones. Focus the analyses on common problems where existing bulk formulations perform poorly—such as over surface heterogeneity, in weak winds, and in very strong winds.
4. Develop a unified algorithm for predicting the turbulent air-sea surface fluxes that spans the environmental range in our datasets and obeys theoretical principles.

APPROACH

This project is a collaboration between Ed Andreas and Larry Mahrt. Dean Vickers of Oregon State University is a contractor on the project. Mahrt has focused on boundary-layer processes in weak winds, when stratification and surface heterogeneity are important issues and when models tend to perform poorly. Andreas, in contrast, has been concentrating on high winds, when sea spray is an important agent for heat and moisture transfer. Vickers brings expertise in processing large datasets—especially, aircraft data—and in parameterizing air-sea exchange. Together, we are developing flux parameterizations that span wind speeds from near zero to hurricane-strength.

In light of a new parameterization for the air-sea drag that we described in our last annual report (also Andreas et al. 2012), we have modified the usual equations for parameterizing the *interfacial* air-sea fluxes of momentum (τ , also called the surface stress), latent heat ($H_{L,int}$), sensible heat ($H_{s,int}$), and enthalpy ($Q_{en,int}$). In our formulation, these four equations now read (Andreas et al. 2012)

$$\tau \equiv \rho u_*^2 = \rho [f(U_{N10})]^2, \quad (1a)$$

$$H_{L,int} = -\rho L_v u_* q_*, \quad (1b)$$

$$H_{s,int} = -\rho c_p u_* \theta_*, \quad (1c)$$

$$Q_{en,int} = -\rho u_* [c_p \theta_* + L_v q_*]. \quad (1d)$$

Here, ρ is the density of moist air; L_v , the latent heat of vaporization; c_p , the specific heat of air at constant pressure; and f , a function that predicts the friction velocity, u_* , from the neutral-stability, 10-m wind speed, U_{N10} . Equation (1a) defines the friction velocity.

The θ_* and q_* in (1b), (1c), and (1d) are flux scales that we compute through Monin-Obukhov similarity:

$$-\theta_* = \frac{k(\Theta_s - \Theta_r)}{\ln(r/z_T) - \psi_h(r/L)}, \quad (2a)$$

$$-q_* = \frac{k(Q_s - Q_r)}{\ln(r/z_Q) - \psi_h(r/L)}. \quad (2b)$$

In these, Θ_s and Q_s are the potential temperature and specific humidity at the surface of the ocean; Θ_r and Q_r , the potential temperature and specific humidity at reference height r ; k , the von Kármán constant ($= 0.40$); z_T and z_Q , the roughness lengths for temperature and humidity, which we compute from the algorithm in Liu et al. (1979; also in Fairall et al. 1996); and ψ_h , an empirical stratification correction that depends on r/L , where L is the Obukhov length.

To account for spray effects, we formulate the *total* scalar fluxes as

$$H_{L,T} = H_{L,int} + H_{L,sp}, \quad (3a)$$

$$H_{s,T} = H_{s,int} + H_{s,sp}, \quad (3b)$$

$$Q_{en,T} = H_{s,int} + H_{L,int} + Q_{en,sp}. \quad (3c)$$

In these, subscript T denotes the total flux across the air-sea interface (presumably, what is measured). The first term on the right [first two terms in (3c)] in each of these is the interfacial flux, parameterized

as in (1) and (2); and the right-most term is the *spray-mediated* flux. Because the spray-mediated fluxes do not scale the same way that the interfacial fluxes do, this separation into spray and interfacial components is crucial in high winds (above about 12 m/s; Andreas 2011).

To address these various ideas, we have assembled a large set of air-sea flux data. We currently have in hand 20 datasets comprising about 7000 air-sea flux measurements. In this set, surface-level wind speeds range from near zero to 72 m/s, and sea surface temperatures range from -1° to 32°C .

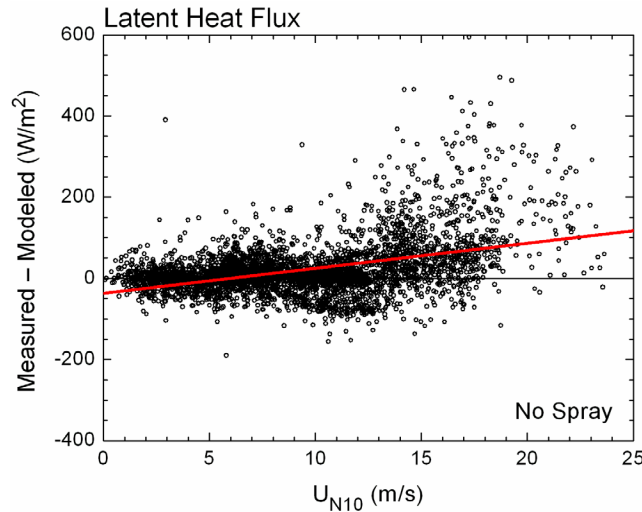


Figure 1. The measured latent heat fluxes are compared with model estimates of the latent heat flux that account for only interfacial transfer. That is, in (3a), the modeled values come from only the $H_{L,int}$ term—a “No Spray” model. The horizontal axis is U_{N10} , the wind speed at 10 m for neutral stability. Notice how the Measured – Modeled values increase with increasing wind speed above 10 m/s. This is the effect of the unmodeled spray-mediated flux. The red line is the best fit through the data and quantifies this dependence on wind speed.

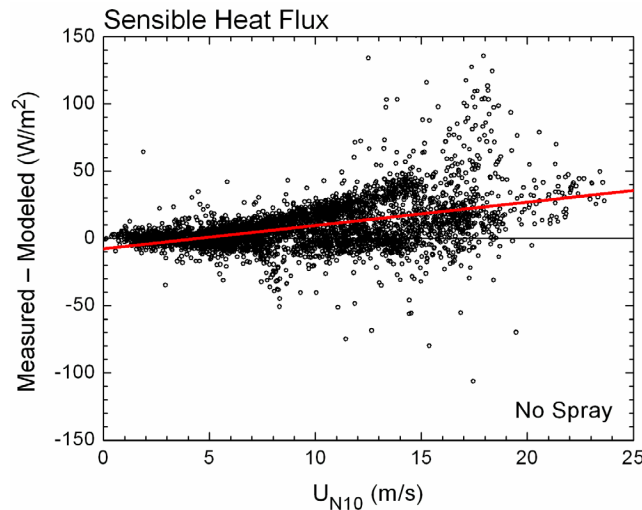


Figure 2. Same as in Figure 1, but this compares measured and modeled sensible heat fluxes, where the modeled sensible heat flux comes from (3b) with only the $H_{s,int}$ term included. Again, the Measured – Modeled values become increasingly positive for U_{N10} above 10 m/s—the signature of spray-mediated transfer.

WORK COMPLETED

Because the interfacial and spray-mediated fluxes in (3) do not scale the same, it is impossible to derive parameterizations for these fluxes from data analysis alone. Rather, our approach has been to develop theoretical models for both the interfacial and spray routes and to validate and tune these models slightly with data. Equations (1) and (2) summarize our theoretical model for the interfacial heat fluxes. We use these parameterizations without further tuning.

Meanwhile, the spray terms ($H_{L,sp}$, $H_{s,sp}$, $Q_{en,sp}$) in our full flux model require extensive microphysically based calculations, as described by Andreas and DeCosmo (2002), Andreas et al. (2008), and Andreas (2010). Using the datasets we have assembled (summarized in Mahrt et al. 2012; Andreas et al. 2012; Vickers et al. 2013), we can evaluate this hypothesized flux algorithm.

Before we consider the spray-mediated fluxes, however, we must ask, “Do we really need to?” The interfacial components of our flux algorithm, (1) and (2), after all, derive from the widely used COARE algorithm (Fairall et al. 1996, 2003). But Figures 1 and 2 show that these components alone do not do well in explaining the data.

Both figures show the measured flux minus the modeled flux as a function of U_{N10} —the neutral-stability, 10-m wind speed. With this format, we can assess both the model bias and the wind speed dependence of that bias. In both figures, the model bias is small for U_{N10} of 10 m/s and less, where the COARE algorithm has been well validated (e.g., Fairall et al. 1996; Grant and Hignett 1998; Chang and Grossman 1999).

At higher wind speeds, on the other hand, both modeled fluxes are systematically smaller than the measured fluxes with increasing wind speed. This behavior is evidence of spray-mediated transfer (e.g., Andreas and DeCosmo 2002).

Hence, in Figures 3 and 4, we now add the spray terms in (3a) and (3b) to the modeled interfacial fluxes. Here, with minor tuning of the microphysical models for $H_{L,sp}$ and $H_{s,sp}$, we have removed the low bias in the modeled flux for all wind speeds in the dataset. That is, with theoretical models that account for both the interfacial and spray routes by which heat and moisture cross the air-sea interface, we explain both the magnitude and the wind speed dependence of the heat fluxes measured in a variety of conditions for wind speeds from near zero to almost 25 m/s.

We have also used our dataset to study the weak-wind regime. For example, we have analyzed all of the aircraft soundings from the CBLAST Weak Wind Pilot Experiment (Mahrt et al. 2013). Our detailed analysis of the structure of the coastal zone boundary layer has concentrated on two case-study days with a large number of vertical profiles measured by the LongEZ (see Figure 5). Flights on 7 August 2001 correspond to a weakly stable boundary layer; flights on 8 August, to a thin, very stable boundary layer. We have made only a rudimentary analysis of the third flight day, which has more chaotic spatial structure.

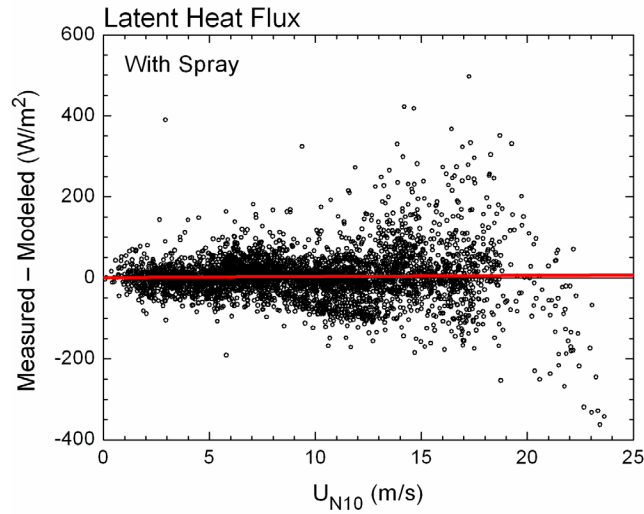


Figure 3. As in Figure 1, but here we add the modeled spray-mediated latent heat flux in (3a). The red line is again the best fit through the data but now is essentially horizontal and coincides with the $y = 0$ line. That is, now the model has explained the magnitude and the wind speed dependence of the measurements.

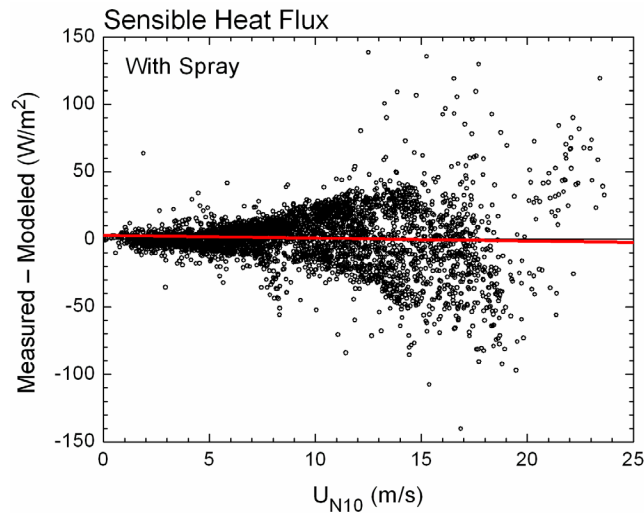


Figure 4. As in Figure 2, but here the modeled flux includes an estimate of the spray-mediated sensible heat flux, $H_{s,sp}$ in (3b). As in Figure 3, the red line—the best fit through the data—is horizontal and essentially along $y = 0$. Therefore, the model has explained both the magnitude and the wind speed dependence of the measurements.

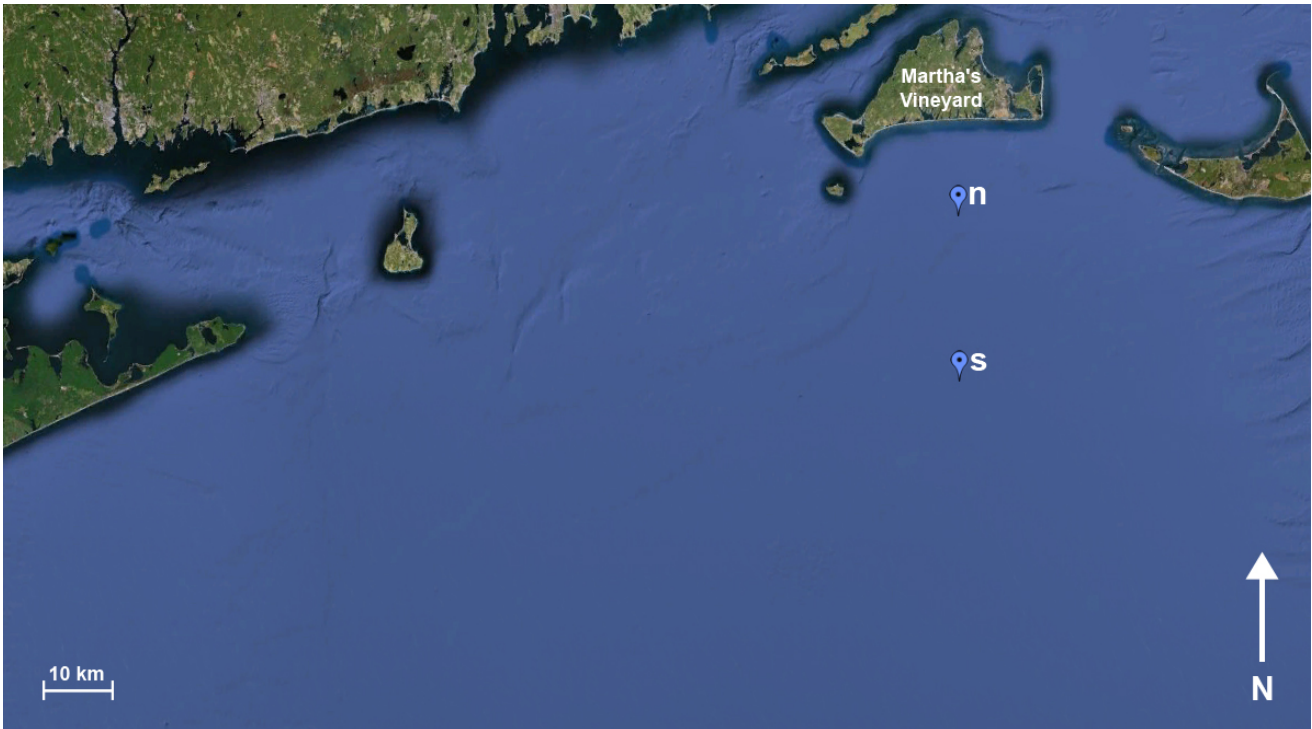


Figure 5. *A map of the observational site where the LongEZ aircraft made slant soundings during the CBLAST Weak Wind Pilot Experiment. Flights on 7 August 2001 were in the vicinity of the southern site (s). Flights on 8 August 2001 were near the southern site in the morning and near the northern site (n) in the afternoon.*

We have also examined the structure of the marine boundary layer off of the coast of Duck, North Carolina, as observed in three separate winter field programs in the late 1990s (SHOWEX). Although the frequency of low-level wind maxima is lower and the number of aircraft soundings is substantially less compared to CBLAST Weak Wind, these data do offer some insight into the vertical structure of the coastal zone boundary layer and will be examined further in the coming year.

Larry Mahrt worked with Gunilla Svennson, Michael Tjernström, and students in Stockholm for a three-week period in May 2013 on possible modification of the COAMPS stable boundary layer package. A large number of sensitivity tests were performed that showed the effects of the rather strict limits on stability in COAMPS. Both the Stockholm group and Shouping Wang of NRL-Monterey plan to investigate modifying these restrictions. Wang is also making COAMPS runs that we will compare with the data from the case studies from the CBLAST Weak Wind Pilot Experiment.

RESULTS

A spray flux algorithm that uses Andreas's full microphysical model to compute $H_{L,sp}$, $H_{s,sp}$, and $Q_{en,sp}$ in (3) is too computer intensive for making routine calculations in large models. Instead, Andreas et al. (2008) observed that droplets whose initial radius is near $50 \mu\text{m}$ contribute most to $H_{L,sp}$ while droplets whose initial radius is near $100 \mu\text{m}$ contribute most to $H_{s,sp}$. Therefore, they used these two droplet classes as bellwethers for their respective spray fluxes. Following Andreas et al. (2008), we therefore parameterize the spray latent heat flux as

$$H_{L,sp} = \rho_w L_v \left\{ 1 - \left[\frac{r(\tau_{f,50})}{50\mu\text{m}} \right]^3 \right\} V_L(u_{*,B}) \quad (4)$$

and the spray sensible heat flux as

$$H_{s,int} = \rho_w c_w (\Theta_s - T_{eq,100}) V_S(u_{*,B}) \quad (5)$$

but use ten times as much data as did Andreas et al. to test these hypotheses.

In (4) and (5), ρ_w is the density of seawater; c_w , the specific heat of seawater; and $u_{*,B}$, the friction velocity from our bulk flux algorithm, (1a). In (4), $\tau_{f,50}$ is the atmospheric residence time of spray droplets that have initial radius $50 \mu\text{m}$. We estimate this as $\tau_{f,50} = H_{1/3} / (2u_{f,50})$ (Andreas 1992), where $H_{1/3}$ is the significant wave height and $u_{f,50}$ is the terminal fall velocity of $50\text{-}\mu\text{m}$ droplets. $r(\tau_{f,50})$ in (4) is then the radius that droplets, originally of radius $50 \mu\text{m}$, have when they fall back into the sea. Andreas et al. (2008) show how we estimate this radius.

In (5), $T_{eq,100}$ is the temperature that droplets with initial radius $100 \mu\text{m}$ reach when given enough time to come to temperature equilibrium in the ambient conditions. This equilibrium temperature is essentially what a tiny, highly curved, saline wet-bulk thermometer would read (Andreas 1995, 1996; Kepert 1996) and, as such, is almost always less than the air temperature.

The V_L and V_S in (4) and (5) are *wind functions* that we evaluate with data. Because the analysis that produced Figures 3 and 4 has yielded $H_{L,sp}$ and $H_{s,sp}$, we can invert (4) and (5) to compute V_L and V_S from data. We use Andreas's (2005) fast algorithms to compute the required microphysical terms, such as $r(\tau_{f,50})$ and $T_{eq,100}$. Figures 6 and 7 show V_L and V_S .

Again, both figures display about 4000 points each, and these points fall consistently along power-law relations. This consistency supports our hypothesized parameterizations, (4) and (5). The fitting lines in the two figures are, respectively,

$$V_L = 1.76 \times 10^{-9} \quad \text{for } 0 \leq u_{*,B} \leq 0.1358 \text{ m/s}, \quad (6a)$$

$$V_L = 2.08 \times 10^{-7} u_{*,B}^{2.39} \quad \text{for } u_{*,B} \geq 0.1358 \text{ m/s}, \quad (6b)$$

and

$$V_S = 3.92 \times 10^{-8} \quad \text{for } 0 \leq u_{*,B} \leq 0.1480 \text{ m/s}, \quad (7a)$$

$$V_S = 5.02 \times 10^{-6} u_{*,B}^{2.54} \quad \text{for } u_{*,B} \geq 0.1480 \text{ m/s}. \quad (7b)$$

In these, V_L , V_S , and $u_{*,B}$ are all in m/s.

Comparing (1) and (2) with (3)–(7) proves how differently the interfacial and spray fluxes scale. A key difference is that $H_{L,int}$ and $H_{s,int}$ are linear in u_* while $H_{L,sp}$ and $H_{s,sp}$ increase, respectively, with u_* to the powers 2.39 and 2.54. This result occurs because whitecaps, which produce most of the spray droplets, increase in coverage at a rate greater than the third power of wind speed.

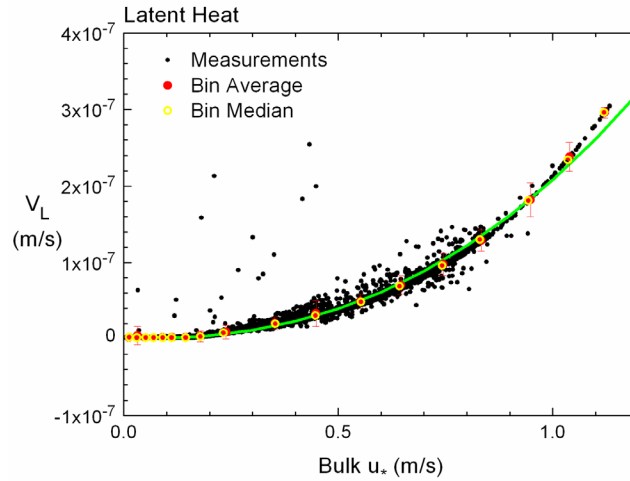


Figure 6. Evaluating the wind function in (4) for the latent heat flux as a function of the bulk friction velocity from (1a). The black circles are individual measurements based on the analysis that produced Figure 3. The red circles are geometric means in bins of $u_{*,B}$; error bars indicate two standard deviations in these bin means. The yellow circles, which generally, are close to the red circles, are bin medians. The green curve, (6), which is a power law relation for large $u_{*,B}$, is the best fit through the data.

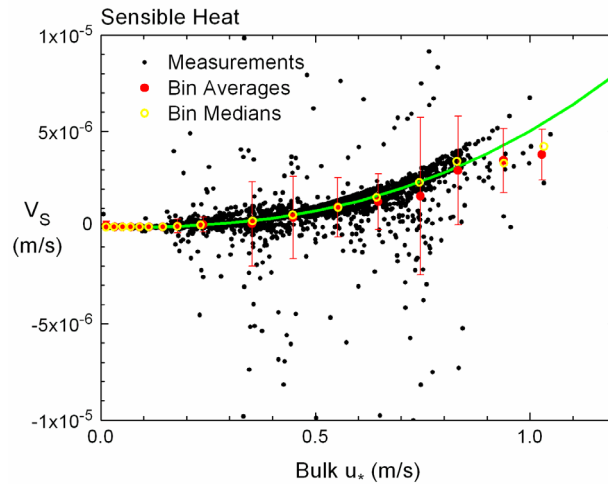


Figure 7. The wind function for the spray sensible heat flux in (5). The horizontal axis is again the bulk friction velocity, $u_{*,B}$. The black circles are individual measurements of this function as deduced from Figure 4. The red and yellow points are the geometric mean and the median within $u_{*,B}$ bins. Error bars are two standard deviations in the bin means. The green curve, (7), is our fit for the wind function for sensible heat.

For the first case-study day of the CBLAST Pilot Experiment (7 August 2001; Figure 5), relatively strong jet speeds of 10–15 m/s occurred at the top of the weakly stable boundary layer at about 100 m above the sea surface. The second case-study day (8 August 2001) is characterized by weaker jet speeds, on the order of 5 m/s, and stronger stability due to advection of warm air from land. The height of the wind maximum is lower, averaging 50 m for the moderately stable regime farther from

the coast (southern site) and averaging 20 m for the very stable regime closer to the coast (northern site). The wind maxima on this day are quite sharp.

We found fluxes computed from the aircraft soundings to be unreliable because they are vulnerable to potentially serious errors; the vertical velocity variance, however, could be adequately evaluated. The relatively deeper (but still shallow) boundary layer and relatively stronger jet farther offshore are consistent with the concept of accelerating flow in a growing stable internal boundary layer downwind from the coast. However, the two sites are not on the same trajectory; and both sites include significant directional shear, precluding definite conclusions.

The low-level jet varies significantly between subsequent soundings on time scales of tens of minutes or less. This variability is evident in Figure 8, which shows wind profiles for the two sites on the second, more stable day. This variability is generally coherent only over small depths. The negative speed shear above the wind maximum is large, and the turbulence at these levels can be significant for individual soundings. The relative variation of the wind and turbulence among the soundings is much greater than that for temperature. Nonetheless, the jet remains persistent within each observational period of several hours.

An inertial mode is probably an important cause of the low-level wind maxima but by itself cannot explain the rapid formation of the wind maxima and its sharpness. A baroclinic mode acts to decelerate the flow near the surface and could enhance the shear on the underside of the wind maximum and also induce wind directional shear. However, the data are inadequate for isolating these mechanisms, but combining COAMPS simulations with the data analysis would be useful.

IMPACT/APPLICATIONS

One of our goals is to develop Fortran code for a bulk air-sea flux algorithm that couples the ocean and atmosphere through flux boundary conditions. Andreas et al. (2008) presented our first version of that code. The analyses and results described in the last three sections are the basis for the next version of that algorithm.

We have been debugging and testing the new code this summer. Figure 9 shows a sample of its predictions. As with most such algorithms, inputs are sea surface temperature and salinity; barometric pressure; and surface-level values of wind speed, air temperature, and humidity. Besides the heat fluxes plotted in Figure 9, our algorithm also predicts the surface stress or friction velocity ($u_{*,B}$) and both the interfacial and spray components of the enthalpy, salt, and freshwater fluxes (Andreas 2010).

Figure 9 emphasizes a conclusion from the last section: While both interfacial fluxes, $H_{L,int}$ and $H_{s,int}$, increase almost linearly with wind speed [see (2a) and (2b)], the spray fluxes, $H_{L,sp}$ and $H_{s,sp}$, increase as higher powers of wind speed [see (6) and (7)] and eventually dominate the surface fluxes.

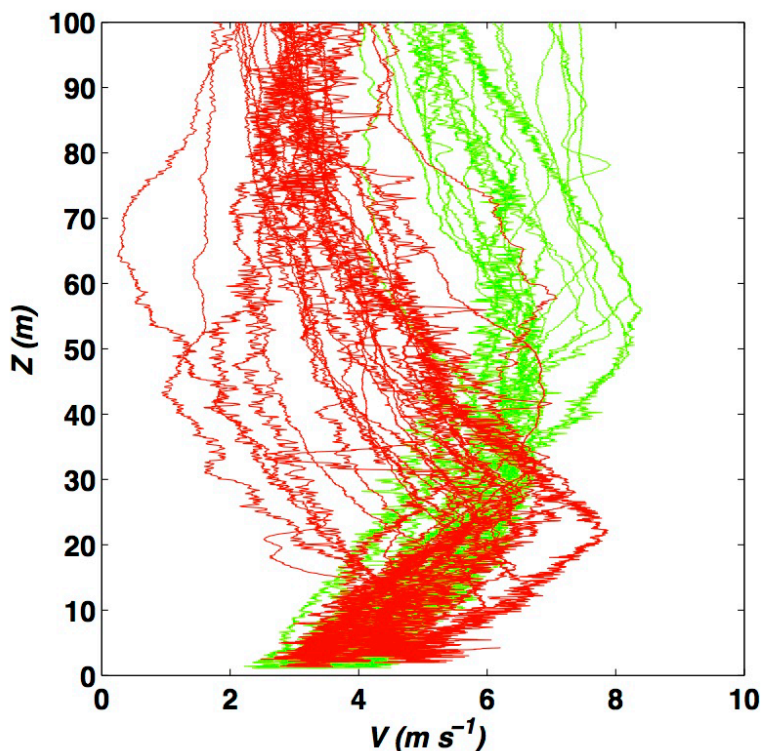


Figure 8. Individual profiles of wind speed on 8 August for the moderately stable regime at the southern CBLAST site (green) and for the very stable regime at the northern site (red). (See Figure 5.) Notice how much sharper and lower the jets are in the very stable regime.

Our work on the vertical structure of the coastal zone boundary layer off of the East Coast of the U.S. reveals a different type of low-level wind maximum than for the extensively studied jets on the West Coast. Since the East Coast jets are often close to the surface and frequently quite sharp, predicting them is more challenging than predicting the West Coast jets. Preliminary results show that models predict East Coast jets, which are often associated with advection of warm air over cooler water, to be too high and too weak.

TRANSITIONS

Journal articles and conference presentations document our work on air-sea exchange. Andreas has also developed a software “kit” that contains instructions and the Fortran programs necessary to implement the bulk air-sea flux algorithm described by Andreas et al. (2008) and Andreas (2010). The current version of that code is 3.4, and the kit is posted at <http://www.nwra.com/resumes/andreas/software.php>, where it can be freely downloaded. Once we are confident in our Fortran algorithms for the revised version of our code, Version 4.0, we will likewise post it to this site.

Meanwhile, early in this reporting year, we supplied NRL-Monterey modelers code for a preliminary bulk flux algorithm that included only our new drag relation, (1a), and algorithms for the interfacial fluxes, (1b)–(1d) and (2). NRL has been testing this algorithm in NAVGEM, the Navy’s global model, and has had promising results.

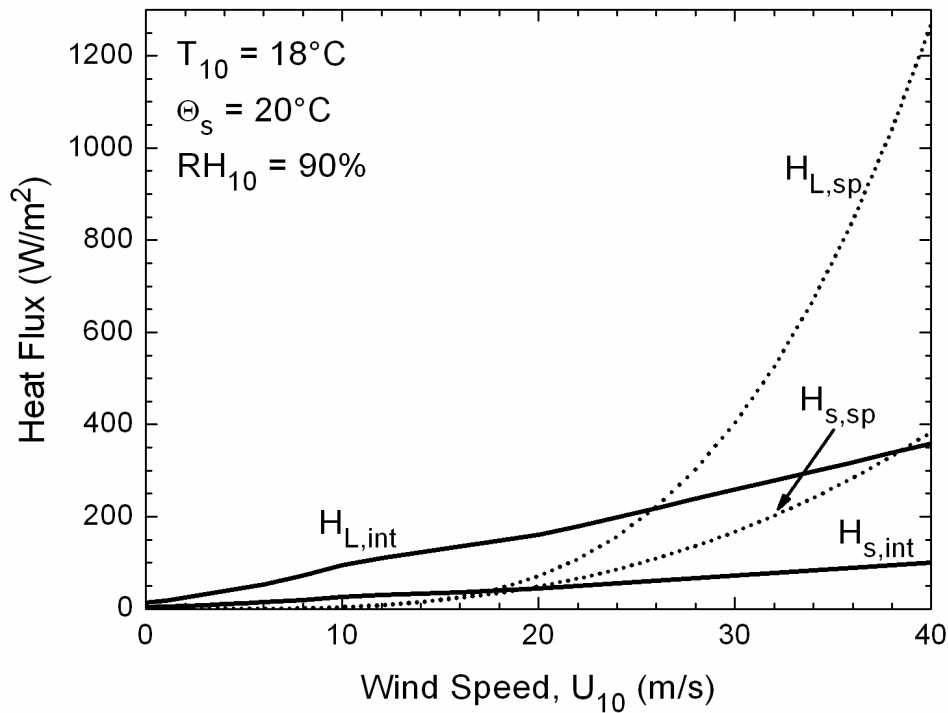


Figure 9. Sample calculations to demonstrate our new bulk flux algorithm.

The plot depicts estimates of the interfacial ($H_{L,int}$ and $H_{s,int}$) and spray-mediated ($H_{L,sp}$ and $H_{s,sp}$) latent and sensible heat fluxes as functions of the wind speed at 10 m, U_{10} , for speeds from 0 to 40 m/s. Other conditions are fixed such that surface temperature (Θ_s) is 20°C, air temperature at 10 m (T_{10}) is 18°C, relative humidity at 10 m (RH_{10}) is 90%, barometric pressure is 1000 mb, surface salinity is 34 psu, and water depth is 3000 m. Both the interfacial latent and sensible heat fluxes are approximately linear in wind speed; each spray flux, however, increases nonlinearly with wind speed and, therefore, eventually overtakes its corresponding interfacial flux in the wind speed range 20–27 m/s.

Because of this existing arrangement with NRL-Monterey modelers, they, of course, will be some of the first scientists to whom we will send our full Version 4.0. We will also send the new code to modelers elsewhere who have expressed interest in using our ideas to couple the atmosphere and ocean in mesoscale and weather forecasting models. In particular, because both the interfacial and spray components of our algorithm are theoretically based and tuned with data, we believe our code can be extrapolated to hurricane-strength winds, where the spray-mediated fluxes may mitigate persistent problems in forecasting hurricane intensity.

RELATED PROJECTS

Andreas and Kathy Jones of the Army’s Cold Regions Research and Engineering Laboratory started in FY12 a project to study spray icing of offshore structures that is funded under ONR’s Arctic program. In January 2013, we carried out a month-long field program on Mt. Desert Rock, a small, well-exposed island 24 miles out into the Atlantic from Bar Harbor, Maine.

During that experiment, we made continuous measurements of the air-sea surface fluxes using eddy-covariance instruments, observed the sea spray size distribution and concentration with a cloud imaging probe, and sampled spray droplets with coated glass slides. The flux measurements will add to the inventory of such measurements that we have assembled under the current project, and the spray observations will provide insight into the spray generation function that is crucial to our calculating V_L and V_S in the current project.

REFERENCES

- Andreas, E. L., 1992: Sea spray and the turbulent air-sea heat fluxes. *J. Geophys. Res.*, **97**, 11,429–11,441.
- Andreas, E. L., 1995: The temperature of evaporating sea spray droplets. *J. Atmos. Sci.*, **52**, 852–862.
- Andreas, E. L., 1996: Reply. *J. Atmos. Sci.*, **53**, 1642–1645.
- Andreas, E. L., 2005: Approximation formulas for the microphysical properties of saline droplets. *Atmos. Res.*, **75**, 323–345.
- Andreas, E. L., 2010: Spray-mediated enthalpy flux to the atmosphere and salt flux to the ocean in high winds. *J. Phys. Oceanogr.*, **40**, 608–619.
- Andreas, E. L., 2011: Fallacies of the enthalpy transfer coefficient over the ocean in high winds. *J. Atmos. Sci.*, **68**, 1435–1445.
- Andreas, E. L., and J. DeCosmo, 2002: The signature of sea spray in the HEXOS turbulent heat flux data. *Bound.-Layer Meteor.*, **103**, 303–333.
- Andreas, E. L., P. O. G. Persson, and J. E. Hare, 2008: A bulk turbulent air-sea flux algorithm for high-wind, spray conditions. *J. Phys. Oceanogr.*, **38**, 1581–1596.
- Andreas, E. L., L. Mahrt, and D. Vickers, 2012: A new drag relation for aerodynamically rough flow over the ocean. *J. Atmos. Sci.*, **69**, 2520–2537.
- Chang, H.-R., and R. L. Grossman, 1999: Evaluation of bulk surface flux algorithms for light wind conditions using data from the Coupled Ocean-Atmosphere Response Experiment (COARE). *Quart. J. Roy. Meteor. Soc.*, **125**, 1551–1588.
- Fairall, C. W., E. F. Bradley, D. P. Rogers, J. B. Edson, and G. S. Young, 1996: Bulk parameterization of air-sea fluxes for Tropical Ocean-Global Atmosphere Coupled-Ocean Atmosphere Response Experiment. *J. Geophys. Res.*, **101**, 3747–3764.
- Fairall, C. W., E. F. Bradley, J. E. Hare, A. A. Grachev, and J. B. Edson, 2003: Bulk parameterization of air-sea fluxes: Updates and verification for the COARE algorithm. *J. Climate*, **16**, 571–591.
- Grant, A. L. M., and P. Hignett, 1998: Aircraft observations of the surface energy balance in TOGA-COARE. *Quart. J. Roy. Meteor. Soc.*, **124**, 101–122.
- Kepert, J. D., 1996: Comments on “The temperature of evaporating sea spray droplets.” *J. Atmos. Sci.*, **53**, 1634–1641.
- Liu, W. T., K. B. Katsaros, and J. A. Businger, 1979: Bulk parameterization of air-sea exchanges of heat and water vapor including the molecular constraints at the interface. *J. Atmos. Sci.*, **36**, 1722–1735.

- Mahrt, L., D. Vickers, E. L. Andreas, and D. Khelif, 2012: Sensible heat flux in near-neutral conditions over the sea. *J. Phys. Oceanogr.*, **42**, 1134–1142.
- Mahrt, L., D. Vickers, and E. L. Andreas, 2013: Low-level wind maxima in the stably stratified coastal zone. *J. Appl. Meteor. Climatol.*, submitted.
- Vickers, D., L. Mahrt, and E. L. Andreas, 2013: Estimates of the 10-m neutral sea surface drag coefficient from aircraft eddy-covariance measurements. *J. Phys. Oceanogr.*, **43**, 301–310.

PUBLICATIONS

- Andreas, E. L., 2012: Book review: *Time Series Analysis in Meteorology and Climatology: An Introduction*. *Bulletin of the American Meteorological Society*, **93**, 1417–1419. [published]
- Andreas, E. L., R. E. Jordan, L. Mahrt, and D. Vickers, 2012: More on the Bowen ratio over saturated surfaces. Extended abstract, *20th Symposium on Boundary Layers and Turbulence*, Boston, MA, 9–13 July 2012, American Meteorological Society, paper 14A.3, 10 pp. [published]
- Andreas, E. L., L. Mahrt, and D. Vickers, 2012: A new drag relation for aerodynamically rough flow over the ocean. *Journal of the Atmospheric Sciences*, **69**, 2520–2537. [published, refereed]
- Andreas, E. L., L. Mahrt, and D. Vickers, 2012: A new drag relation for aerodynamically rough flow over the ocean. Extended abstract, *18th Conference on Air-Sea Interaction*, Boston, MA, 9–12 July 2012, American Meteorological Society, paper 3.2, 19 pp. [published]
- Andreas, E. L., R. E. Jordan, L. Mahrt, and D. Vickers, 2013: Estimating the Bowen ratio over the open and ice-covered ocean. *Journal of Geophysical Research*, **118**, doi:10.1002/jgrc.20295. [in press, refereed]
- Jones, K. F., and E. L. Andreas, 2012: Sea spray concentrations and the icing of fixed offshore structures. *Quarterly Journal of the Royal Meteorological Society*, **138**, 131–144. [published, refereed]
- Mahrt, L., D. Vickers, E. L. Andreas, and D. Khelif, 2012: Sensible heat flux in near-neutral conditions over the sea. *Journal of Physical Oceanography*, **42**, 1134–1142. [published, refereed]
- Mahrt, L., D. Vickers, and E. L. Andreas, 2013: Low-level wind maxima in the stably stratified coastal zone. *Journal of Applied Meteorology and Climatology*. [refereed]
- Vickers, D., L. Mahrt, and E. L. Andreas, 2013: Estimates of the 10-m neutral sea surface drag coefficient from aircraft eddy-covariance measurements. *Journal of Physical Oceanography*, **43**, 301–310. [published, refereed]